MAX-PLANCK-INSTITUT FÜR PLASMAPHYSIK

GARCHING BEI MÜNCHEN

SELF-SPUTTERING AND REFLECTION

W. Eckstein

IPP 9/54 August 1985

Die nachstehende Arbeit wurde im Rahmen des Vertrages zwischen dem Max-Planck-Institut für Plasmaphysik und der Europäischen Atomgemeinschaft über die Zusammenarbeit auf dem Gebiete der Plasmaphysik durchgeführt.

IPP 9/54 W. ECKSTEIN SELF-SPUTTERING AND REFLECTION

Abstract

Selfsputtering and reflection are investigated with the Monte Carlo program TRIMSP. The results include particle and energy reflection coefficients, sputtering yields and sputtered energy versus incident angle and energy. Angular and energy distributions of reflected and sputtered particles are also given. Reflection and sputtering values are compared to show their contributions to selfsputtering. A comparison of calculated sputtering yields and sputtering efficiencies (sputtered energy) with experimental data is carried out. The systems investigated are mainly the bombardment of C , Ni, and W with self-ions.

1. Introduction

Sputtering of amorphous and polycrystalline targets has been studied for a long time experimentally and theoretically. Recent surveys by Andersen and Bay /1/ and by Sigmund /2/ should be mentioned for a representation of the field and the earlier literature. Recently also Monte Carlo computer simulations /3/ have been shown to describe sputtering phenomena quite successfully. This paper is restricted to selfsputtering, where target atoms and incident ions are the same species. In this case the measured data do not distinguish between sputtering and reflection. It is assumed that the contribution of reflected particles to the sputtering yield and the reflected energy to the sputtered energy /1/ is small for a mass ratio, $M_2/M_1 = 1$, of the target mass to ion mass. Böttiger et al. /4/ showed indeed that the reflection coefficient for $M_2/M_1 = 1$ is of the order of 1 % (range from 4 % to 0.4 % due to different potentials), whereas the sputtering yield is of the order of 1 in the keV-range for normal incidence. For increasing angle of incidence the reflection coefficient is increasing /4/, whereas the sputtering yield for large angles of incidence is decreasing, so that for grazing incidence reflection exceeds sputtering. This has been shown by Robinson /5/ in a computer simulation of selfsputtering of Uranium.

In this paper the Monte Carlo program TRIMSP is used to investigate more quantitatively selfsputtering and reflection. The sputtering yield will be compared to the particle reflection coefficient, the sputtered energy to the reflected energy, the mean energy of sputtered particles to the mean energy of reflected particles. In addition the angular and energy

distributions of sputtered and reflected particles are studied to find out, if there is a possibility to distinguish experimentally between sputtered and reflected particles. Comparisons with available experimental and theoretical data are carried out.

2. The computational model

For the evaluation of the various quantities the Monte Carlo simulation program TRIM SP (version TRSP1C) is used. The program is described extensively in Ref. /3/, so that only a few essential points are mentioned here: The program is based on the binary collisional model and assumes a randomised target. As interaction potential the Kr-C potential /6/ is applied, for the inelastic energy loss a 50% - 50 % modus of the non-local Lindhard-Scharff /7/ and the local Oen-Robinson /8/ models is used. If not stated otherwise, no non-local inelastic energy loss outside the uppermost atomic layer is taken into account. For identical projectile and target atoms the surface binding energy is applied to sputtered as well as reflected particles. The surface binding energies for the different targets are taken from tables /9/. In all calculations a planar surface potential is assumed, which leads to a gain of the surface binding energy for the incident particles and an equal loss of energy for the leaving particles and in addition to a refraction of the incident particles as well as the outgoing reflected and sputtered particles. The calculations cannot give any information on the charge state of the outgoing particles.

The results include the following quantities:

R_N	the particle reflection coefficient, defined as the fraction of incident particles which is reflected; the R_E energy reflection coefficient, defined as the fraction of the incident energy which is carried by the reflected particles;
$\bar{E}_{refl.}/E_o = R_E/R_N$	the relative mean energy of the reflected particles (E_o is the incident particle energy);
Y	the sputtering yield, defined as the number of sputtered particles per incident particles;
Y_E	the sputtered energy, defined as the energy carried by the sputtered particles divided by the incident energy;
$\bar{E}_{sputt.}/E_o = Y_E/Y$	the relative mean energy of the sputtered particles.

In addition, angular and energy distributions of reflected and sputtered particles were calculated.

The number of histories (number of incident particles) was chosen such that the angular and energy distributions exhibit reasonable statistics or, in the case of reflection coefficients (which were the smaller quantities),

such that the number of reflected particles was at least 100. One should keep in mind that in experiments of self-sputtering usually the sums $R_N + Y$ and $R_E + Y_E$ are measured. The energy distributions may give some indication of the contribution of reflected particles. It should be noted that spike effects in sputtering /2/ are neglected. These may have some influence in the case of heavy species, such as W.

The paper deals with ion-target combinations, where both ion and target atoms are identical. One example each of a light, medium and heavy species, was chosen: C, Ni and W. Choosing identical ion and target atoms implies that both reflected and sputtered particles experience the same surface binding energy and that no compositional changes occur in the target. Both effects, different binding energies for different species in compound targets and dose dependent surface concentration changes present special difficulties which are discussed in /10,11/.

3. Reflection coefficients and sputtering yields

a) Normal incidence

In Fig.1 the reflection coefficients and the relative mean energy of reflected particles are plotted versus the incident energy for normal incidence. The species are C, Ni and W, as in all subsequent data. All reflection coefficients show a maximum. The energy position of the maximum depends on the value of the surface binding energy and on the species as in sputtering. The maximum position for Ni increases with the surface binding energy from 0.15 keV for an assumed surface binding energy, E_s = 1 eV, to about 2 keV for E_s = 10 eV. The maximum values of the particle reflection

coefficient are in the order of 1 %. The values of the calculated particle reflection coefficients are in reasonable agreement with earlier theoretical data /4/. The relative mean energy does not vary much, less than a factor of two. The absolute values of the relative mean energy are of the order of a few per cent of the incident energy, which is about an order of magnitude lower than for the light ions /12/.
The sputtering yield ,Y, the sputtered energy, Y_E, and the mean energy of the sputtered particles versus the incident energy at normal incidence are given in Fig. 2. Y and Y_E show a strong increase at low energies. The maximum of Y depends on the species, and the maximum of Y_E is reached at lower energies than that of Y. Therefore the Y_E values are decreasing already at lower energies, leading to a monotonous decrease of the relative mean energy with incident energy. For Ni and W a comparison with experimental data /13-16/ demonstrates good agreement. This implies that spike effects are not of great importance in the energy range investigated. The discrepancy of a factor of 2 for carbon /17, 18/ is also observed for other incident particles. Agreement with experimental data can be obtained by choosing a surface binding energy of about 4 eV. If a reduced binding energy or some other effect /18/ is the real cause for the discrepancy is not clear at the moment.

A comparison of the reflection data and the sputtering data, see Fig. 3, shows that the sputtering yields are more than an order of magnitude larger than the particle reflection coefficients over the whole energy range investigated. From these data it can be concluded that in a self-sputtering experiment at normal incidence the reflected particles can at low energies (below 100 eV) contribute up to 10 % to the measured sputtering yield.

The ratio of the energy reflected to the energy sputtered is larger and less strongly dependent on the incident energy, than the ratio of the particle reflection to the sputtering yield. The mean energy of the reflected particles is larger than the mean energy of the sputtered particles. The ratio of the mean energies $\overline{E}_{refl.}/\overline{E}_{sputt.}$ is increasing with increasing incident energy.

Fig. 4 demonstrates that the particle and energy reflection coefficients scale with ε but only for ε-values much larger than the ε-values corresponding to the respective surface binding energies. The same is true for the so called sputtering efficiency, /19/, $\gamma = R_E + Y_E$ (see fig.5). An approximate ε-scaling for γ was shown in /20/ for $10^{-2} < \varepsilon < 3$. The experimental data /20/ and theoretical data, taken from Winterbon's tables /21/ give larger values for γ. The discrepancy of the calculated values of γ in this paper to Andersen's data /20/ for Pb is less than a factor of two for most of the energy range covered. It should be mentioned that the calculated and measured sputtering yields for Ni and W are in much better agreement (see fig.2) and do not show the systematic deviation as for γ. Different models for the inelastic energy loss, no inelastic loss or 100 % Lindhard-Scharff, change the sputtering efficiency by less than 10 %. An increase in Y and Y_E by about 40 % and in R_N and R_E by about 20 % (at the same incident energy above 1 keV for U) is obtained by using the so called "universal potential" of Ziegler et al. /22/. In this paper the Firsov screening length is used, whereas for the experimental data the Lindhard screening is applied. The Firsov ε is about 10 % smaller than the Lindhard, so that the experimental curves have to be shifted. Taking this difference into account, the Pb-data /20/ are in reasonable agreement with the calculated data. The deviations for the Cu-data /20/ are much larger.

But here it has to be mentioned that Cu shows a larger sputtering yield as compared to neighbouring elements as for example Ni. The surface binding energies for Ni and Cu differ by 25 % but the sputtering yield for Cu is more than a factor of 2 larger than the yield for Ni. This situation is similar for Ag and Au. These large yields for Cu, Ag, Au cannot be understood by simple collisional considerations. Therefore a program based on binary collisions gives too small yields for Cu, if it gives the right values for Ni. From this fact it is expected that the experimental sputtering efficiency for Cu is larger by a factor of 2 to 3 than the calculated ones. A similar reason could be also possible for the somewhat larger experimental Pb-data. If a deviation for the sputtering efficiencies for Ni and W between calculated and measured data is observed despite the fact that the sputtering yields are in good agreement than a closer comparison between calculated and measured total energy distributions has to be performed.

The mean energy of the leaving particles is given by $\gamma E_o = R_N \bar{E}_{refl.} + Y \bar{E}_{sputt}$ /4/. The first term on the right side of the equation contributes about 15 % at 100 eV and about 5 % at 10^4 eV as can be determined from Fig. 1-3. The mean energy of the sputtered particles determined by the measured value of γ gives higher values /23/ because of the above mentioned discrepancy between the calculated and measured values of γ . The ratio of the relative mean energies of reflected to sputtered particles indicates that in the energy distributions of reflected particles the contribution of higher energy particles must be of greater importance than in the distribution of the sputtered particles.

b) Non-normal incidence

The reflection coefficients and the relative mean energy of the reflected particles versus the angle of incidence, α, are shown in fig. 6, for 0.1 and 1 keV. All three quantities show an increase with increasing angle of incidence, to about unity. The shapes of the curves depend somewhat on the incident energy and the species but the curves are similar for the examples investigated. At glancing incidence the mean energy of the reflected particles approaches the incident energy, E_o.

The sputtering yield and the sputtered energy versus the angle of incidence are shown in Fig. 7. All exhibit a maximum (cf. also Ref. /3/) between 50^o and 70^o depending on the species. In the energy range investigated, 0.1 and 1 keV, it seems to be more pronounced for the lighter elements. Also the relative mean energy of the sputtered particles shows a maximum for Ni and W (1 keV), but not for C and W (0.1 keV), where it keeps increasing with angle of incidence. A comparison between the particle reflection coefficient and the sputtering yield shows that both quantities become comparable at an angle of incidence of about 55^o at an incident energy of 0.1 keV and at about 80^o for 1 keV, Fig. 8. For the energy reflection coefficient and the sputtered energy this occurs at an even lower angle of incidence, viz. at about $\alpha = 40^o$ for 0.1 keV and $\alpha = 65^o$ for 1 keV. Above these angles the reflection coefficients are larger than the sputtering quantities. This result indicates that in self-sputtering experiments the reflection makes an important contribution at non-normal incidence and becomes the dominant contribution at grazing incidence. Furthermore, the contribution of the reflection is more important in the energy coefficients (R_E, Y_E) than in the number quantities (R_N, Y) as can be seen in Fig. 8. In

Fig. 8 the ratios R_N/Y, R_E/Y_E and $\bar{E}_{refl.}/\bar{E}_{sputt.}$ are shown versus the angle of incidence. It is apparent that the mean energy of reflected particles, $\bar{E}_{refl.}$, is larger than the mean energy of the sputtered particles, $\bar{E}_{sputt.}$, for all angles of incidence. In fact, the ratio $\bar{E}_{refl.}/\bar{E}_{sputt.}$ increases with increasing angle of incidence.

It should be noted that at low incident energies the particle reflection coefficient does not reach unity at grazing incidence. This fact could already be seen in Fig. 6e. The reason for this effect, given in /5/ is, that due to the surface binding energy, E_s, the maximum effective angle of incidence, α', is limited:

$$\alpha' = \arccos\left(E_s/(E_s+E_o)\right)^{1/2}$$

The absolute value of the reflection coefficients also depends on the model of inelastic energy losses at the surfaces. In all data calculated for this paper, no non-local inelastic energy loss outside the uppermost target atoms was taken into account /3/. If such a non-local inelastic energy loss for a distance (1.58 A for W) of half a lattice constant above the surface is applied, the reflection coefficients are reduced by about 25 % which gives better correspondence to the values calculated in /5/. The quantitative picture is only slightly changed, and the conclusions drawn above are still valid, because the sputtering yields are reduced by about the same amount /3/.

The dependence of the sputtering efficiency, $\gamma = R_E + Y_E$, versus the angle of incidence, α, is given in Fig. 9 for two examples. The comparison of the calculated γ with Sigmund's formula /eq. (81b) in 24/ shows good

agreement for $\varepsilon = 0.13$, whereas at $\varepsilon = 4.5 \times 10^{-4}$ the calculations give larger values than the formula.

4. Angular Distributions

a) Normal incidence

The angular distributions of the reflected particles are shown in Fig. 10, for incident energies between 0.1 and 3 keV. The plot chosen (the distribution versus the cosine of the emission angle, β) is due to Robinson /5/, and makes for easy comparison with a cosine distribution, which is represented by the straight line starting from 2 on the ordinate scale (the starting point is determined by the number of cosine-intervals chosen). The distributions exhibit an under-cosine structure at low energies, an over-cosine structure at higher energies and a cosine structure somewhere between. The energy region, where a cosine distribution appears, increases with target mass.

The angular distributions of the sputtered particles, shown in Fig. 11, are very similar to those of the reflected particles. The only difference is, that at higher energies the reflected particles tend towards an over-cosine distribution, whereas the sputtered particles still show a distribution very close to cosine.

b) Non-normal incidence

For 1 keV C onto C the angular distributions of reflected particles become increasingly non-cosine with increasing angle of incidence, α, Fig. 12a. As expected from simple considerations and light ion scattering data /12/ the

distributions move to a more specular reflection. Contrary to the result for reflected particles, the angular distributions of sputtered particles show no strong dependence on the angle of incidence, only a slight deviation to an under-cosine distribution with increasing angle of incidence, Fig. 12b. This result can explain the differences between the reflection coefficients and sputtering yields versus the angle of incidence (reflected particles at grazing incidence will retain most of their initial energy).

5. Energy Distributions

a) Normal incidence

The energy distributions of reflected and sputtered particles are shown in Fig. 13, for incident energies between 0.1 and 3 keV. As stated in Sect. 3a, the intensity of the reflected particles is at least one order of magnitude lower than the intensity of sputtered particles. Both distributions show about the same energy cut-off at the high energy end, where both distributions come closer together. The maximum of the distribution of the reflected particles is less clearly developed and occurs at higher energies than for the distribution of sputtered particles. In the distribution of reflected particles the statistics for energies below 1 eV become very poor. It was also found that due to the proximity of the cut-off energy (for the maximum transferrable energy) the maximum of the distribution of the sputtered particles at low incident energies may occur below half the surface binding energy /2/. It should be remembered that these distributions include all sputtered and reflected particles

resp., and that the distributions in different emission directions may differ slightly. The distributions of both reflected and sputtered particles cover the same energy range, so that it will be nearly impossible to distinguish reflected and sputtered particles from their energy distribution.

b) Non-normal incidence

With increasing angle of incidence the high energy tail in the distributions of the reflected particles becomes more important, as seen in Fig. 14 for 1 keV C bombardment of C. At lower energies the distribution of reflected particles becomes nearly constant with increasing angle of incidence, whereas the high energy end of the distribution of sputtered particles shows a slight shift to higher energies with increasing α . It should again be mentioned that the energy distributions change markedly with emission angles /3/. Here only the total distributions are given. At grazing incidence nearly all particles leaving the target are reflected ones.

6. Conclusions

In the energy range above 100 eV the contribution of reflected particles to the selfsputtering yield is less than about 10 % and decreasing with increasing energy for normal incidence. The same holds for the reflected energy in comparison with the sputtered energy. The mean energy of the sputtered particles is smaller than the mean energy of reflected particles.

The calculated sputtering yields for Ni and W show good agreement with experimental data. For C a deviation is observed, which may be due to a lower surface binding energy.

-scaling for the reflection coefficients and the sputtering efficiency is observed for energies well above the surface binding energy E_s. The calculated sputtering efficiency is always lower than experimental and theoretical curves with an increasing deviation to higher energies. With increasing angle of incidence the reflection becomes more important in comparison to sputtering and is dominant at grazing incidence. Andersen's formula for the sputtering efficiency gives good agreement with the calculated data at not too low energies.

Angular distributions for reflected particles show small deviations from a cosine distribution, whereas sputtered particles give better agreement at normal incidence. For nonnormal incidence sputtered particles still show a distribution very close to cosine, whereas the reflected particles become more peaked in the forward direction with increasing angle of incidence. In contrast to the energy distributions of sputtered particles, reflected particles do not exhibit a pronounced maximum and the distributions of both kind of particles are similar at the high energy tail for normal incidence. For nonnormal incidence the energy distributions of reflected particles become rather flat, showing a pronounced maximum at the high energy end only for grazing incidence.

Acknowledgements

The critical reading of the manuscript by J. Roth and helpful discussions with J. Bohdansky and W. Möller are gratefully acknowledged.

REFERENCES

/1/ H.H. Andersen, H. Bay in Topics in Applied Physics, Vol. 47, p. 145, Springer-Verlag Berlin, Heidelberg, 1981.

/2/ P. Sigmund in Sputtering by Particle Bombardment I, ed. R. Behrisch, Springer-Verlag, Berlin, 1981.

/3/ H.J. Biersack, W. Eckstein, Appl. Phys. A34 (1984) 73

/4/ J. Böttiger, J.A. Davies, P. Sigmund, K.B. Winterbon, Rad. Eff. 11 (1971) 69

/5/ M.T. Robinson, J. Appl. Phys. 54 (1983) 2650

/6/ W. Wilson, L. Haggmark, J.P. Biersack, Phys. Rev. B15 (1977) 2458

/7/ J. Lindhard, M. Scharff, Mat. Fys. Medd. Dan. Vid. Selsk, 27 (1953) 15

/8/ O.S. Oen, M.T. Robinson, Nucl. Instr. Meth. 132 (1976) 647

/9/ R. Hultgren, J.P. Desai, D.T. Hawkins, M. Gleiser, K.K. Kelley, D.D. Wagman, Selected Values of the Thermodynamic Properties of the Elements (Am. Soc. Metals, Metals Park, Ohio,USA 1973).

/10/ W. Eckstein, F.P. Biersack, Appl. Phys. A 37 (1985)1

/11/ W. Eckstein, W. Möller, Nucl. Instr. Meth. B 7/8 (1985)727

/12/ R.A. Langley, J. Bohdansky, W. Eckstein, P. Mioduszewski, J. Roth, E. Taglauer, E.W. Thomas, H. Verbeek, K.L. Wilson, Nuclear Fusion, Special Issue 1984, IAEA Vienna STI/PUB/23/SPI/1984, p. 12

/13/ A. Fontell, E. Arminen, Can. J. Phys. 47 (1969) 2405

/14/ E. Hechtl, H.L. Bay,J. Bohdansky, Appl. Phys. 16 (1978) 147

/15/ O. Almen, G. Bruce, Nucl. Instr. Meth. 11 (1961) 257 & 279

/16/ M. Saidoh, K. Sone, Jap. J. Appl. Phys. 22 (1983) 1361

/17/ E. Hechtl, J. Bohdansky, J. Roth, J. Nucl. Mater. 103 & 104 (1981) 333

/18/ J. Roth, Nuclear Fusion, Special Issue 1984, IAEA Vienna STI/PUB/23/SPI/1984, p. 72.

/19/ P. Sigmund, Can. J. Phys. 46 (1968) 731

/20/ H.H. Andersen, Rad. Eff. 7 (1971) 179

/21/ K.B. Winterbon, Ion Implantation Range and Energy Deposition Distributions, Vol. 2, IFI/Plenum, New York, 1975

/22/ J.F. Ziegler, J.P. Biersack, U. Littmark, IBM Research Report RC 9250, Yorktown, USA, 1982

/23/ H.H. Andersen, Rad. Eff. 3(1970) 51

/24/ P. Sigmund, Phys. Rev. 184 (1969) 383

Figure captions

Fig.1 Particle (R_N) and energy (R_E) reflection coefficients and the relative mean energy of the reflected particles, $\overline{E}_{refl.}/E_o$, versus the incident energy, E_o, for normal incidence, $\alpha = 0^o$.
(a) C→C, (b) Ni→Ni, (c) W→W

Fig.2 Sputtering yield, Y, sputtered energy, Y_E, and the relative mean energy of the sputtered particles, $\overline{E}_{sputt.}/E_o$ versus the incident energy, E_o for normal incidence, $\alpha = 0^o$.
(a) C→C, (b) Ni→Ni, (c) W→W

Fig.3 The ratios R_N/Y, R_E/Y_E and $\overline{E}_{refl.}/\overline{E}_{sputt.}$ versus the incident energy, E_o, for normal incidence
(a) C→C, (b) Ni→Ni, (c) W→W

Fig.4 Particle and energy reflection coefficients, R_N and R_E, and R_E/R_N, versus the reduced energy, ε, for C, Ni and W.

Fig.5 The sputtering efficiency, $\gamma = R_E + Y_E$, versus the reduced energy, ε, for several elements ($M_2/M_1 = 1$).

Fig.6 Particle and energy reflection coefficients, R_N and R_E, and the relative mean energy of reflected particles, $\overline{E}_{refl.}/E_o$, versus the angle of incidence, α, for the bombardment of
(a) 100 eV C→C, (b) 1 keV C→C, (c) 100 eV Ni→Ni
(d) 1 keV Ni→Ni, (e) 100 eV W→W, (f) 1 keV W→W.

Fig.7 Sputtering yield, Y, sputtered energy, Y_E, and the relative mean energy of sputtered particles, $\bar{E}_{sputt.}/E_o$, versus the angle of incidence, α.

(a) 100 eV C→C, (b) 1 keV C→C, (c) 100 eV Ni→Ni,

(d) 1 keV Ni→Ni, (e) 100 eV W→W, (f) 1 keV W→W

Fig.8 The ratios R_N/Y, R_E/Y_E and $\bar{E}_{refl.}/\bar{E}_{sp.}$ versus the angle of incidence, .

(a) 100 eV C→C, (b) 1 keV C→C, (c) 100 eV Ni→Ni

(d) 1 keV Ni→Ni, (e) 100 eV W→W, (f) 1 keV W→W.

Fig.9 The sputtering efficiency, $\gamma = R_E + Y_E$, versus the angle of incidence, α. Comparison with Sigmund's formula /24,1/.

(a) 1 keV W→W ($\varepsilon = 4.46 \times 10^{-4}$)

(b) 30 keV Ni→Ni ($\varepsilon = 0.129$)

Fig.10 Angular distributions of all reflected particles versus the cosine of the emission polar angle, ß, for normal incidence, $\alpha = 0^o$.

(a) 0 .1, 0.3, 1 and 3 keV C→C

(b) 0.1 and 1 keV Ni→Ni

(c) 0.1 and 1 keV W→W.

Fig.11 Angular distributions of all sputtered particles versus the cosine of the emission polar angle, ß, for normal incidence, $\alpha = 0^o$.

(a) 0.1, 0.3, 1 and 3 keV C→C

(b) 0.1 and 1 keV Ni→Ni

(c) 0.1 and 1 keV W→W.

Fig.12 Angular distributions of (a) reflected and (b) sputtered particles versus the cosine of the emission polar angle, ß, for 1 keV C bombardment of C at four angles of incidence, α.

Fig.13 Energy distributions of reflected and sputtered particles versus the energy, E, of reflected resp. sputtered particles, for normal incidence, $\alpha = 0^{o}$.

(a) 0.1 keV C→C, (b) 0.3 keV C→C, (c) 1 keV C→C

(d) 3 keV C→C. (e) 0.1 keV Ni→Ni, (f) 0.1 keV W→W

(g) 1 keV Ni→Ni, (h) 1 keV W→W.

Fig.14 Energy distributions of reflected and sputtered particles versus the energy, E, of reflected resp. sputtered particles for 1 keV C bombardment of C.

(a) $\alpha = 45^{o}$, (b) $\alpha = 60^{o}$, (c) $\alpha = 70^{o}$, (d) $\alpha = 80^{o}$.

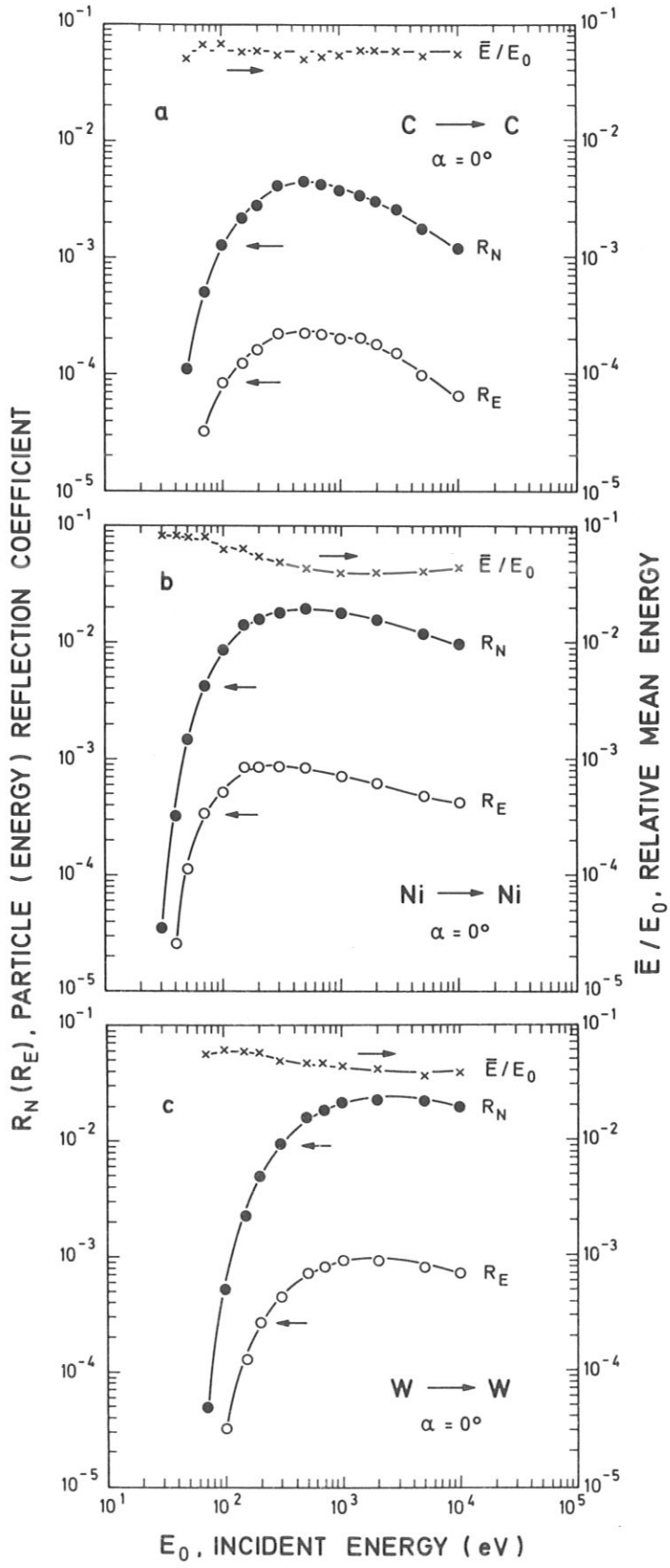
a
C → C
α = 0°
b
Ni → Ni
α = 0°
c
W → W
α = 0°
$\bar{E}/E_0$
R_N
R_E
$R_N(R_E)$, PARTICLE (ENERGY) REFLECTION COEFFICIENT
$\bar{E}/E_0$, RELATIVE MEAN ENERGY
E_0, INCIDENT ENERGY (eV)

Fig. 1

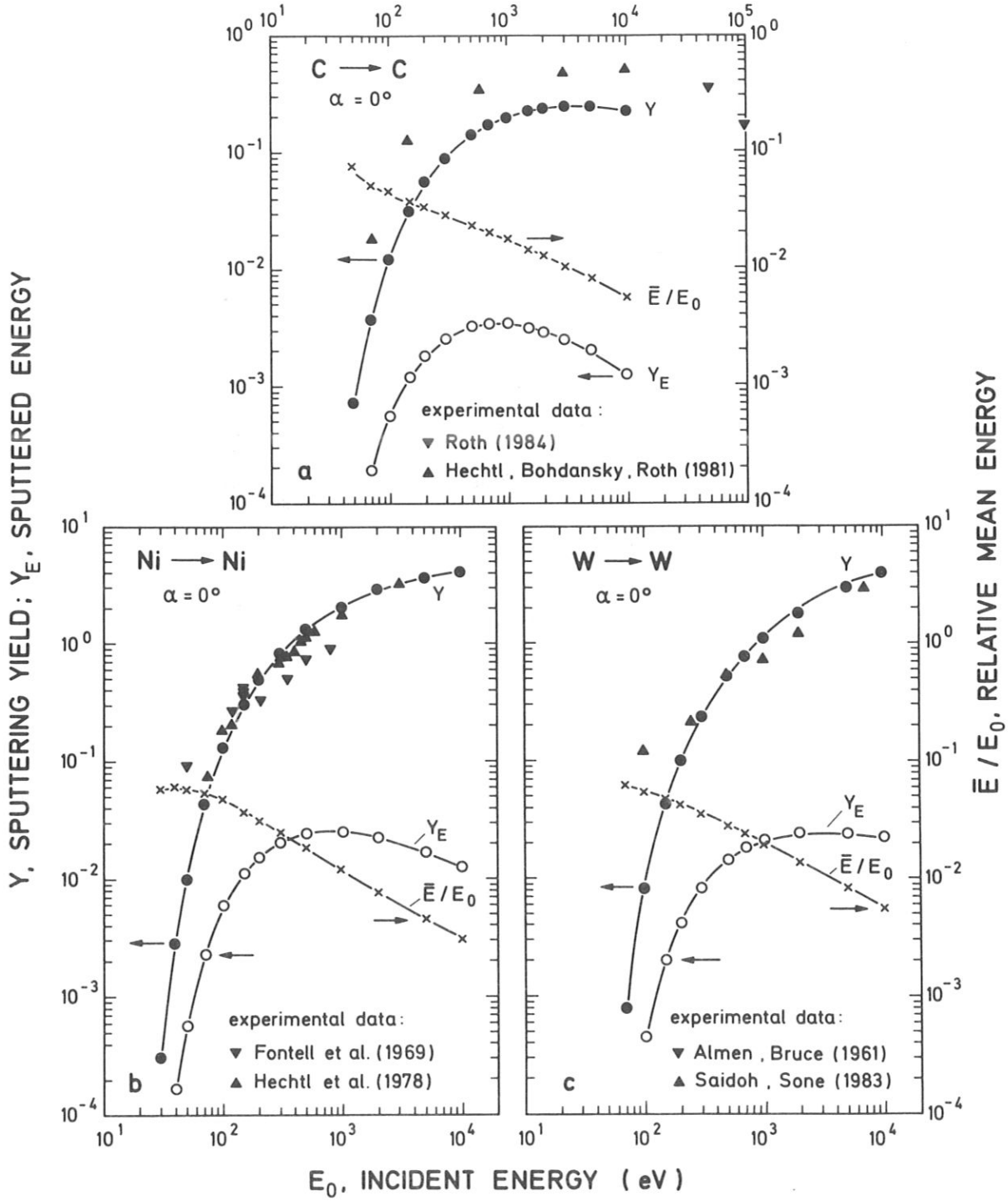
C → C
α = 0°
Y
Ē / E0
YE
experimental data :
Roth (1984)
Hechtl , Bohdansky , Roth (1981)
a
Ni → Ni
α = 0°
Y
YE
Ē / E0
experimental data:
Fontell et al. (1969)
Hechtl et al. (1978)
b
W → W
α = 0°
Y
YE
Ē / E0
experimental data:
Almen , Bruce (1961)
Saidoh , Sone (1983)
c
Y, SPUTTERING YIELD ; YE, SPUTTERED ENERGY
Ē / E0, RELATIVE MEAN ENERGY
E0, INCIDENT ENERGY (eV)

Fig.2

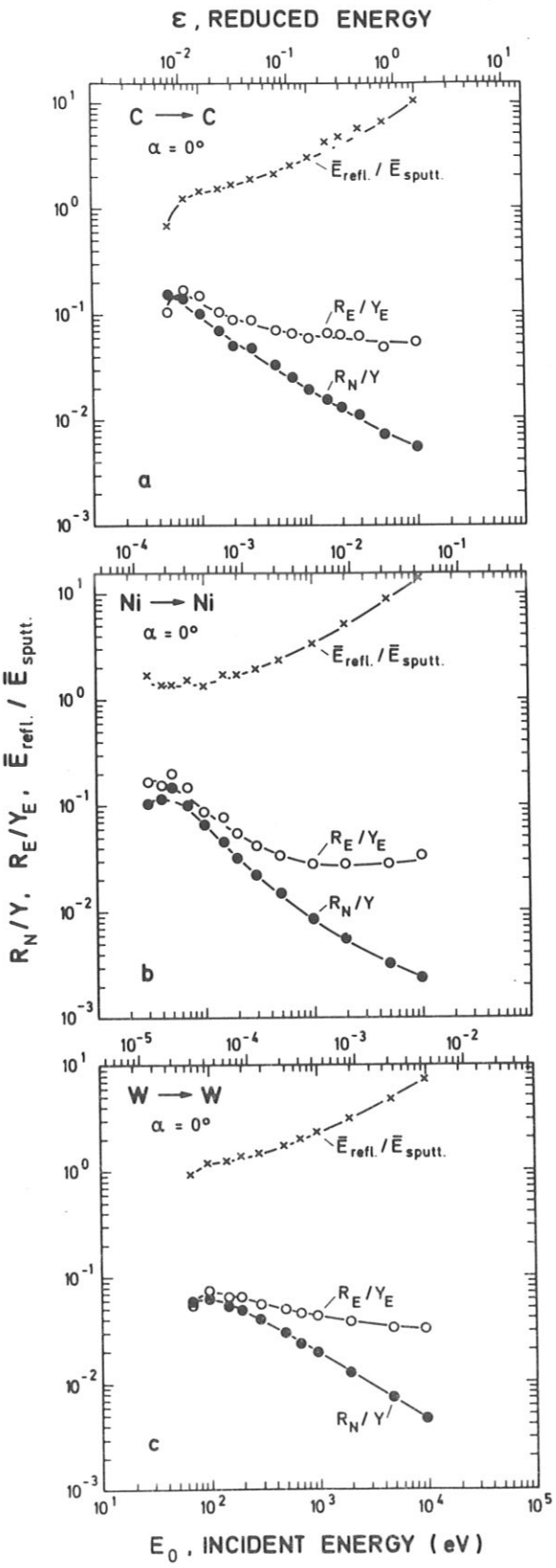
ε , REDUCED ENERGY
C → C
α = 0°
Ē refl. / Ē sputt.
R E / Y E
R N / Y
a
Ni → Ni
α = 0°
Ē refl. / Ē sputt.
R E / Y E
R N / Y
b
W → W
α = 0°
Ē refl. / Ē sputt.
R E / Y E
R N / Y
c
R N / Y, R E / Y E, Ē refl. / Ē sputt.
E 0 , INCIDENT ENERGY (eV)

Fig.3

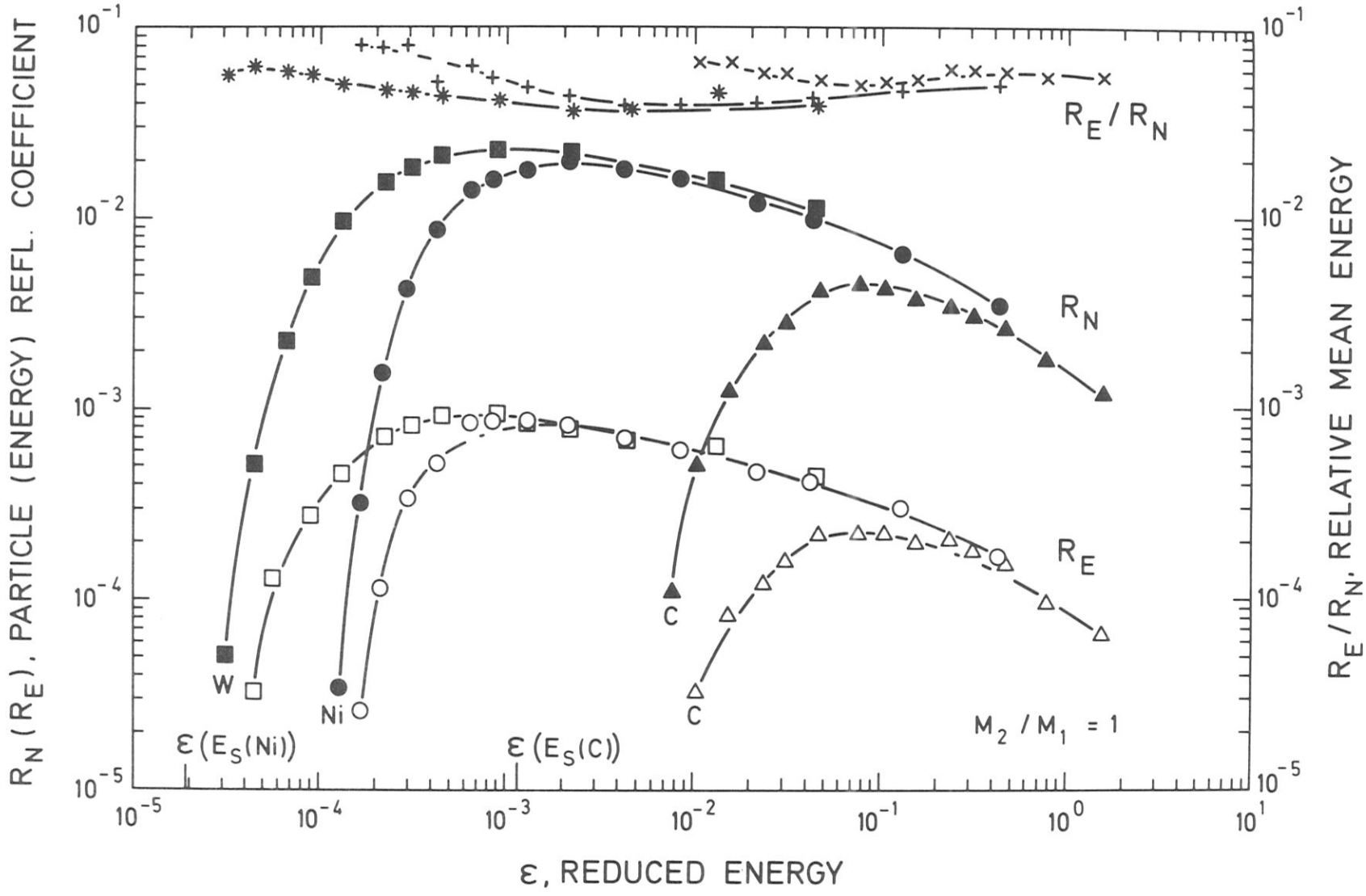
$R_N(R_E)$, PARTICLE (ENERGY) REFL. COEFFICIENT
R_E/R_N, RELATIVE MEAN ENERGY
ε, REDUCED ENERGY
R_E/R_N
R_N
R_E
W
Ni
C
C
$M_2/M_1 = 1$
ε(E_S(Ni))
ε(E_S(C))

Fig. 4

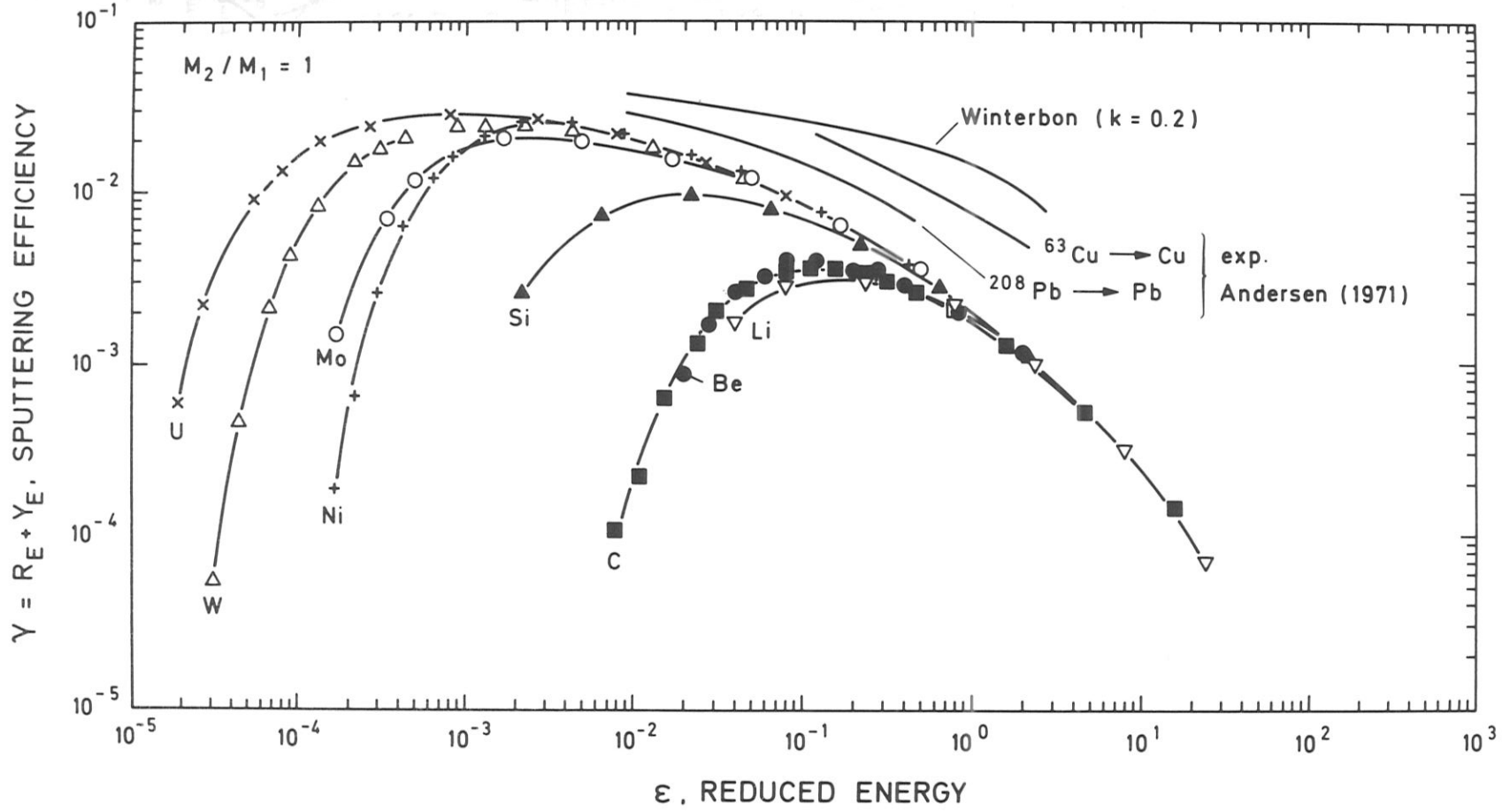
$M_2 / M_1 = 1$
Winterbon (k = 0.2)
$^{63}Cu \rightarrow Cu$
$^{208}Pb \rightarrow Pb$
exp.
Andersen (1971)
U
W
Mo
Ni
Si
Li
Be
C
$Y = R_E + Y_E$, SPUTTERING EFFICIENCY
ε, REDUCED ENERGY
10^{-1}
10^{-2}
10^{-3}
10^{-4}
10^{-5}
10^{-5}
10^{-4}
10^{-3}
10^{-2}
10^{-1}
10^{0}
10^{1}
10^{2}
10^{3}

Fig. 5

a
0.1 keV C → C
b
1 keV C → C
c
0.1 keV Ni → Ni
d
1 keV Ni → Ni
e
0.1 keV W → W
f
1 keV W → W
$\bar{E}/E_0$
R_N
R_E
$R_N(R_E)$, PARTICLE (ENERGY) REFLECTION COEFFICIENT
$\bar{E}/E_0$, RELATIVE MEAN ENERGY
α, ANGLE OF INCIDENCE
0°
30°
60°
90°

Fig.6

a
0.1 keV C → C
b
1 keV C → C
c
0.1 keV Ni → Ni
d
1 keV Ni → Ni
e
0.1 keV W → W
f
1 keV W → W
Y
Y_E
$\bar{E}/E_0$
Y, SPUTTERING YIELD ; Y_E, SPUTTERED ENERGY
$\bar{E}/E_0$, RELATIVE MEAN ENERGY
α, ANGLE OF INCIDENCE
0°
30°
60°
90°

Fig.7

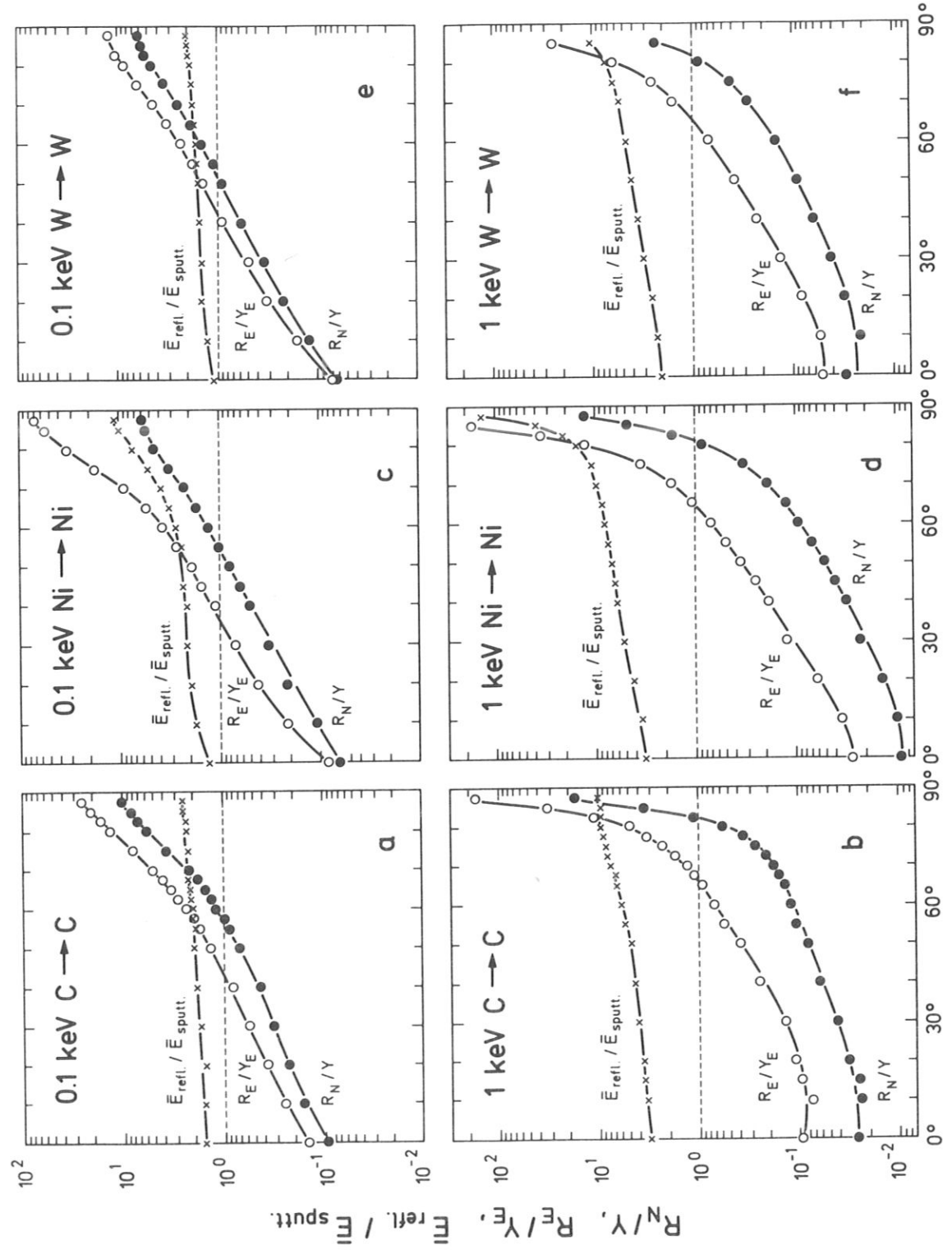
0.1 keV C → C
0.1 keV Ni → Ni
0.1 keV W → W
1 keV C → C
1 keV Ni → Ni
1 keV W → W
$\bar{E}_{refl.} / \bar{E}_{sputt.}$
R_E / Y_E
R_N / Y
a
b
c
d
e
f
R_N/Y, R_E/Y_E, $\bar{E}_{refl.} / \bar{E}_{sputt.}$
10^{2}
10^{1}
10^{0}
10^{-1}
10^{-2}
0°
30°
60°
90°
α, ANGLE OF INCIDENCE

Fig.8

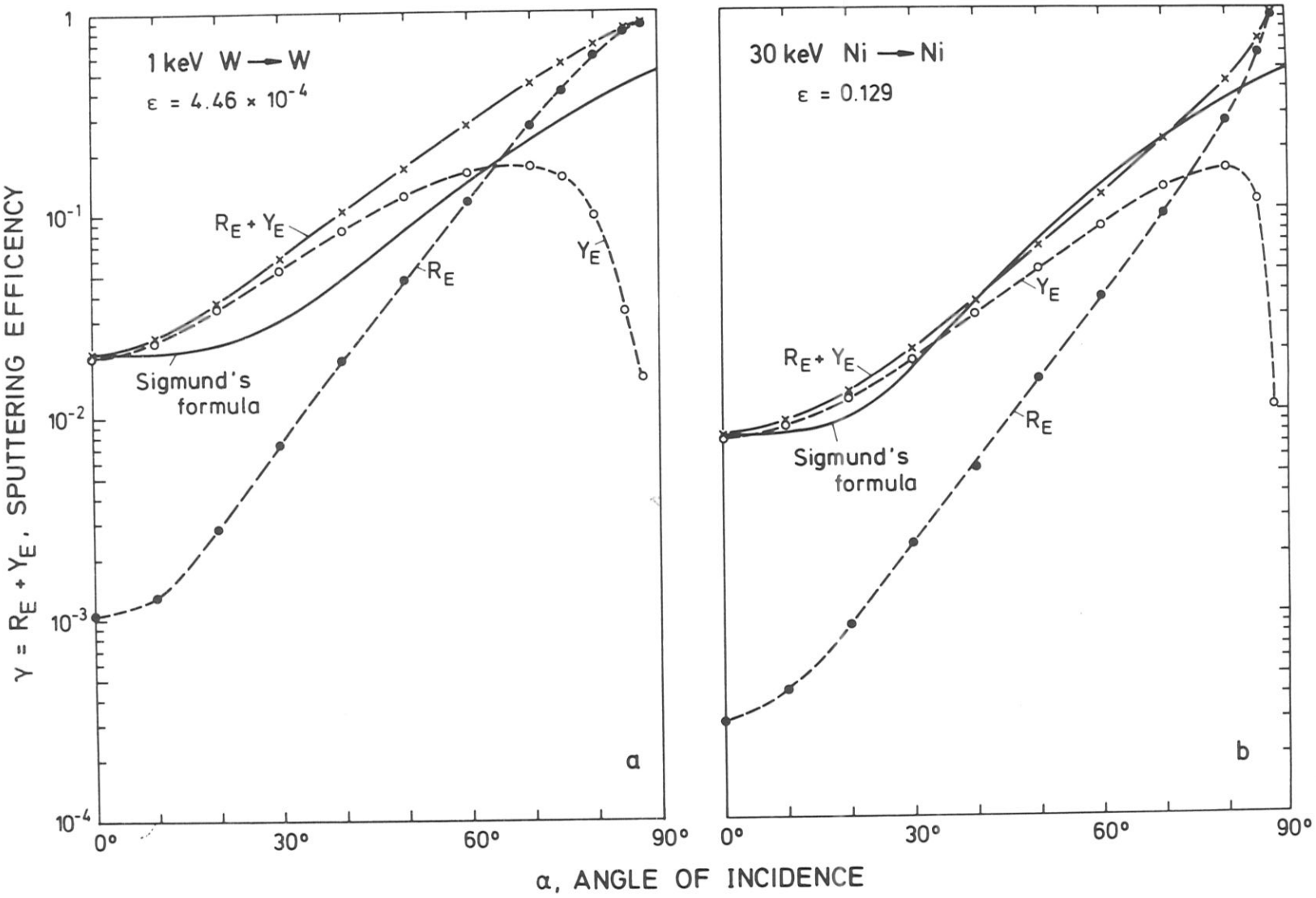
1 keV W → W
ε = 4.46 × 10⁻⁴
R_E + Y_E
Y_E
R_E
Sigmund's formula
a
30 keV Ni → Ni
ε = 0.129
R_E + Y_E
Y_E
R_E
Sigmund's formula
b
γ = R_E + Y_E, SPUTTERING EFFICENCY
1
10⁻¹
10⁻²
10⁻³
10⁻⁴
0°
30°
60°
90°
α, ANGLE OF INCIDENCE

Fig. 9

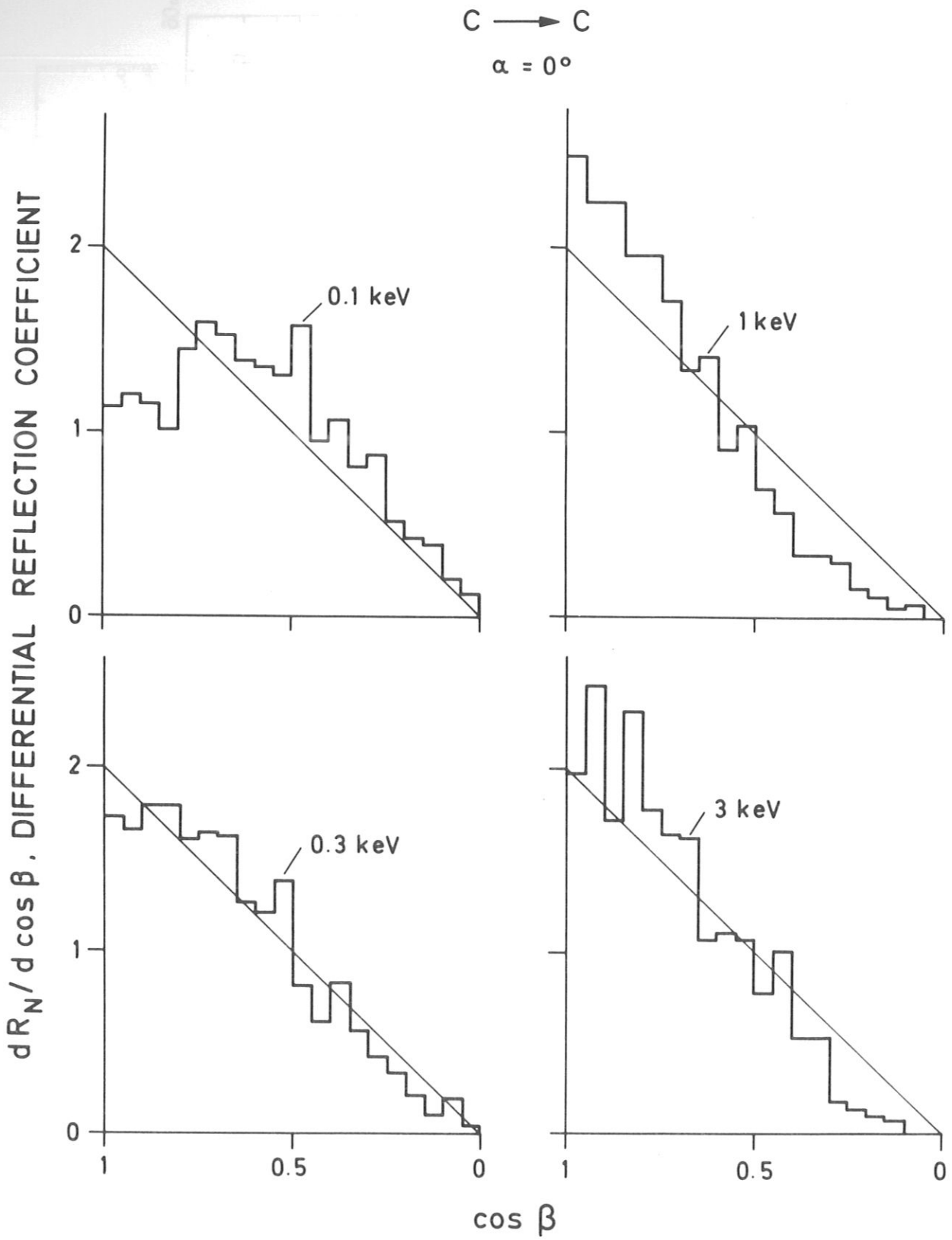
C → C
α = 0°
0.1 keV
1 keV
0.3 keV
3 keV
dR_N / d cos β, DIFFERENTIAL REFLECTION COEFFICIENT
cos β
2
1
0
1
0.5
0

Fig.1oa

Ni → Ni
α = 0°
1 keV
0.1 keV
a
W → W
α = 0°
1 keV
0.1 keV
b
3
2
1
0
0
0.5
1
cos β
dR_N / d cos β · DIFFERENTIAL REFL. COEFFICIENT

Fig.10b and c

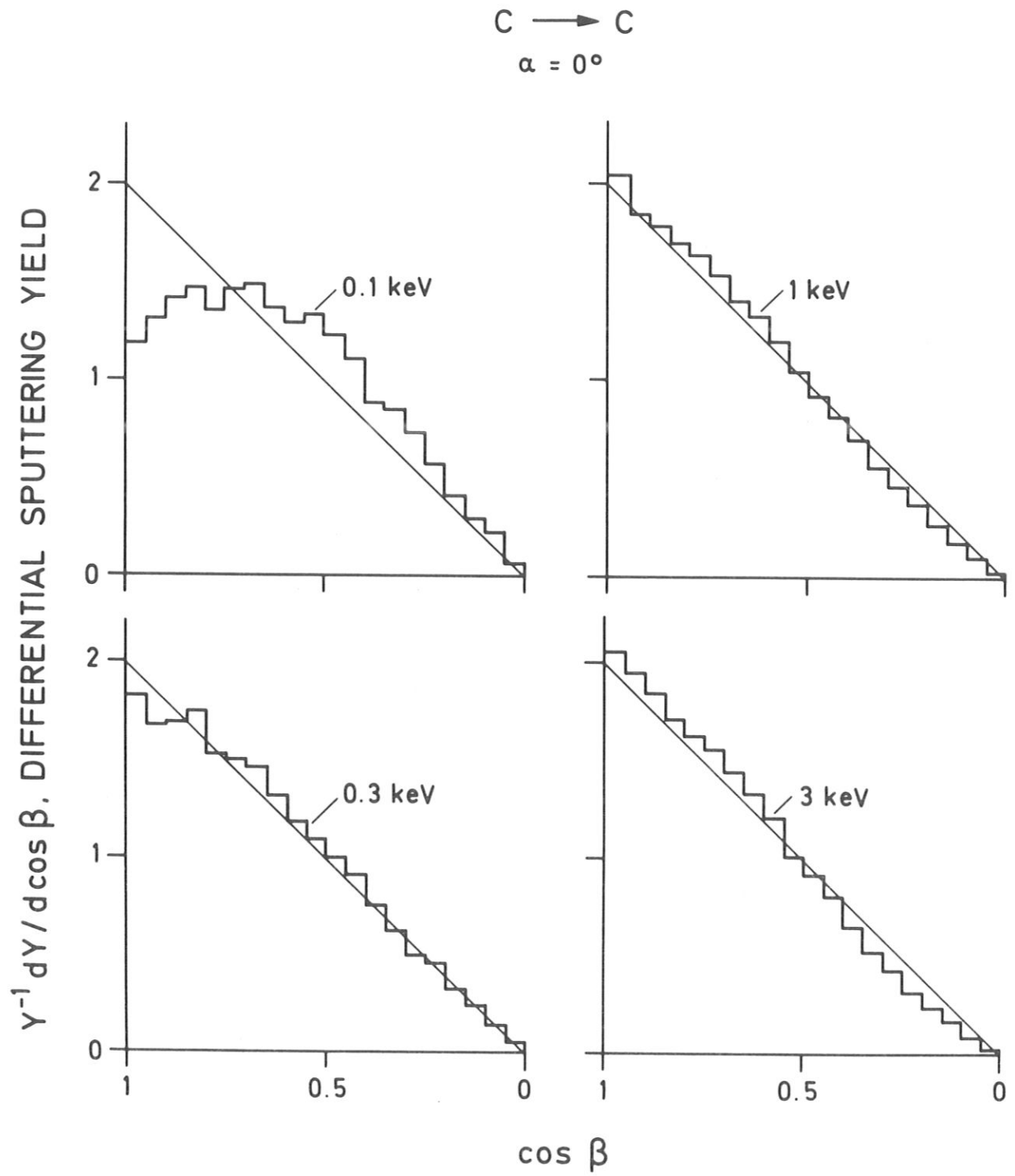
C → C
α = 0°
Y⁻¹ dY/d cos β, DIFFERENTIAL SPUTTERING YIELD
0.1 keV
1 keV
0.3 keV
3 keV
2
1
0
1
0.5
0
cos β

Fig.11a

$\gamma^{-1} \frac{d\gamma}{d \cos \beta}$, DIFFERENTIAL SPUTT. YIELD
Ni → Ni
α = 0°
1 keV
0.1 keV
a
W → W
α = 0°
1 keV
0.1 keV
b
cos β
3
2
1
0
0.5
1

Fig.11b and c

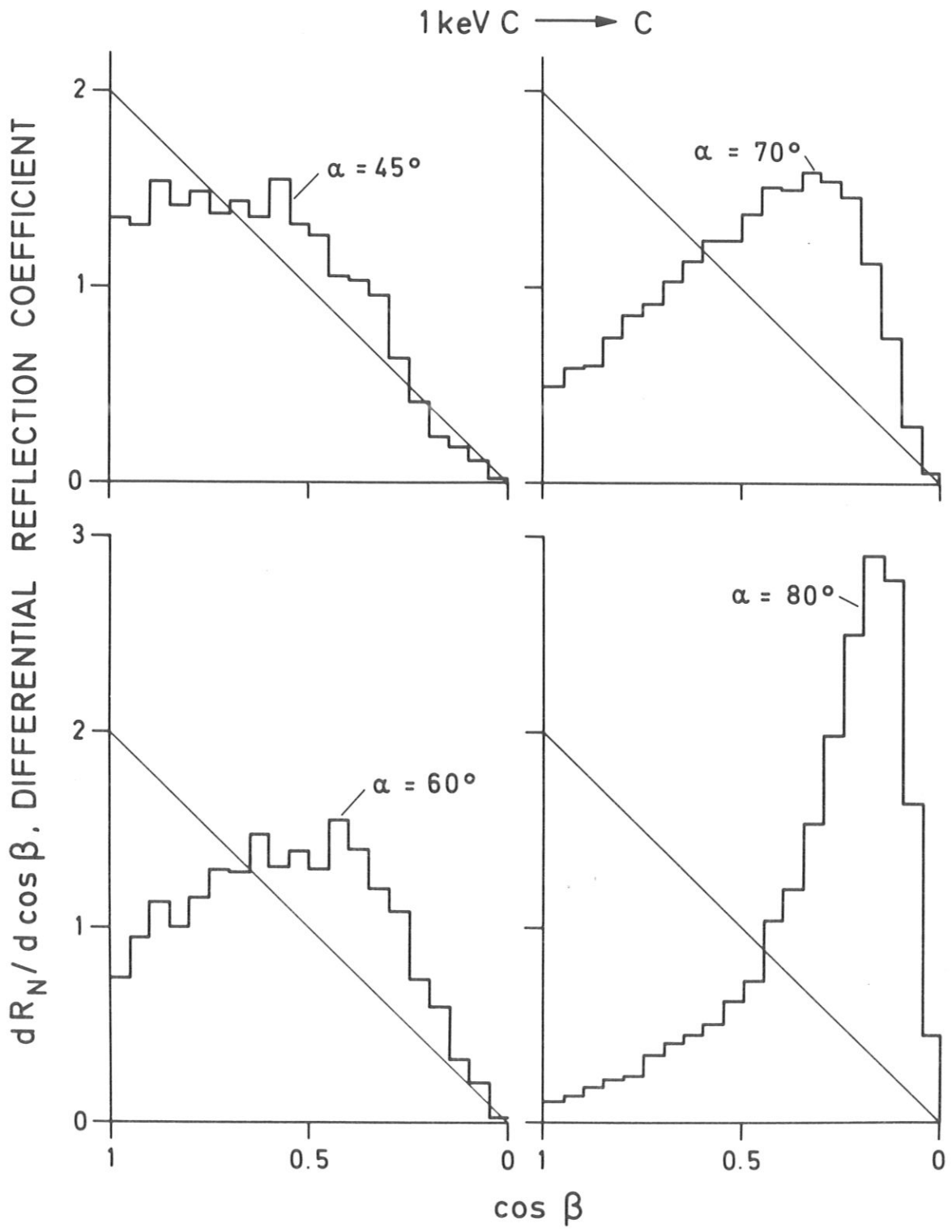
1 keV C → C
α = 45°
α = 70°
α = 60°
α = 80°
dR_N / d cos β, DIFFERENTIAL REFLECTION COEFFICIENT
cos β
0
0.5
1
2
3

Fig.12a

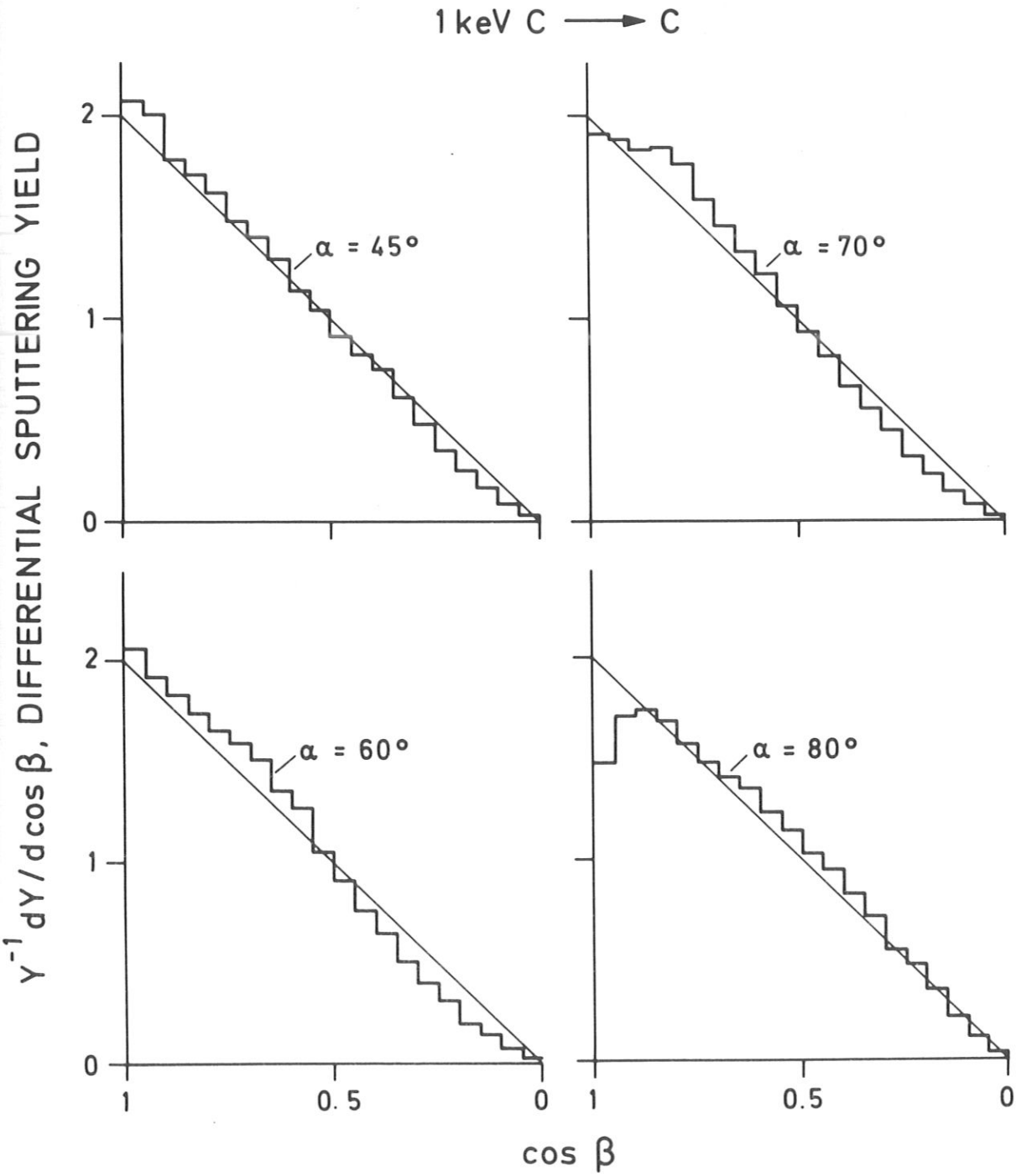
1 keV C → C
α = 45°
α = 70°
α = 60°
α = 80°
2
1
0
1
0.5
0
Y⁻¹ dY/d cos β, DIFFERENTIAL SPUTTERING YIELD
cos β

Fig.12b

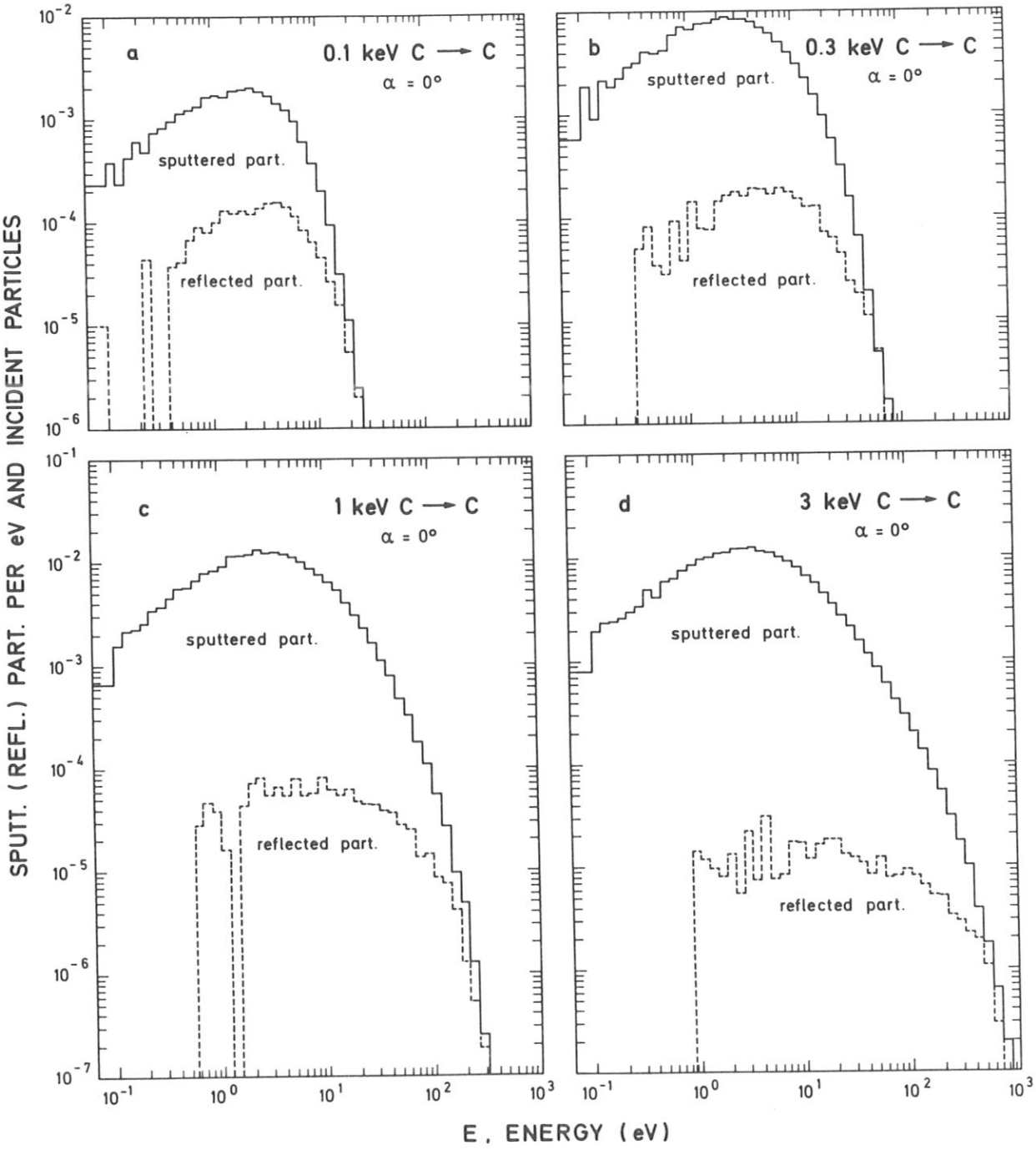
a
0.1 keV C → C
α = 0°
sputtered part.
reflected part.
b
0.3 keV C → C
α = 0°
sputtered part.
reflected part.
c
1 keV C → C
α = 0°
sputtered part.
reflected part.
d
3 keV C → C
α = 0°
sputtered part.
reflected part.
SPUTT. (REFL.) PART. PER eV AND INCIDENT PARTICLES
E, ENERGY (eV)

Fig.13a-d

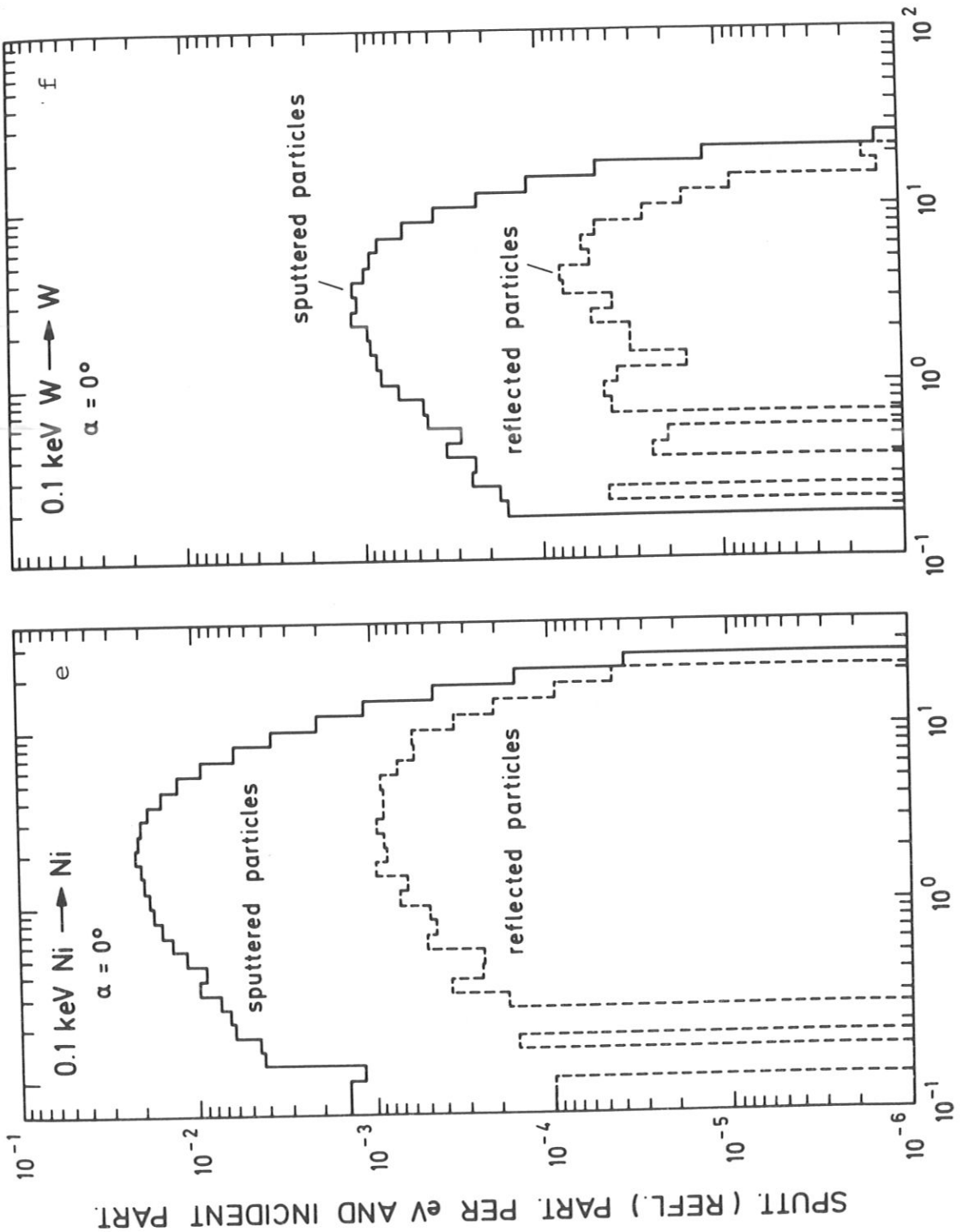
0.1 keV Ni → Ni
α = 0°
e
sputtered particles
reflected particles
0.1 keV W → W
α = 0°
f
sputtered particles
reflected particles
SPUTT. (REFL.) PART. PER eV AND INCIDENT PART.
E, ENERGY (eV)

Fig.13e and f

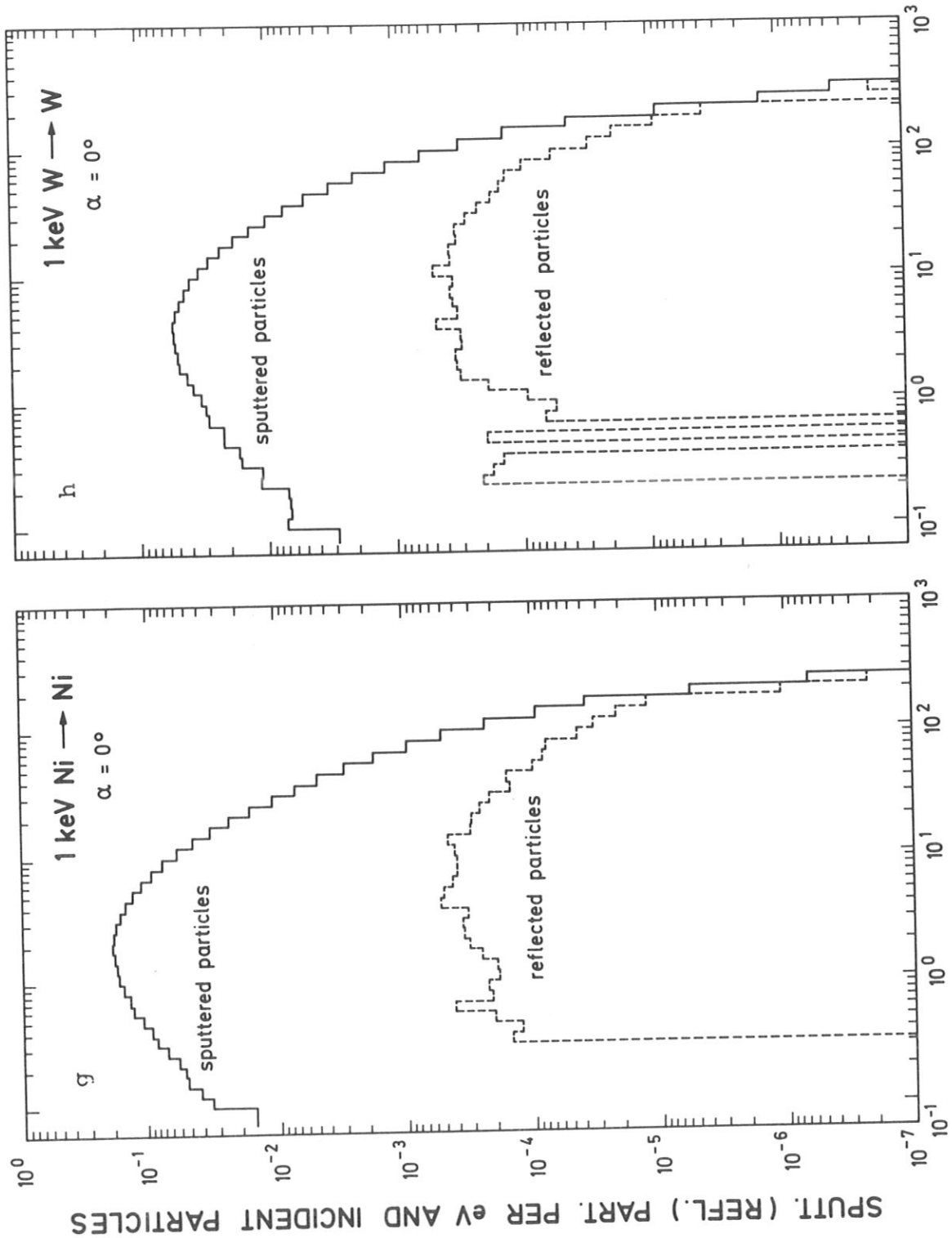
1 keV Ni → Ni
α = 0°
g
sputtered particles
reflected particles
1 keV W → W
α = 0°
h
sputtered particles
reflected particles
SPUTT. (REFL.) PART. PER eV AND INCIDENT PARTICLES
E, ENERGY (eV)

Fig.13g and h

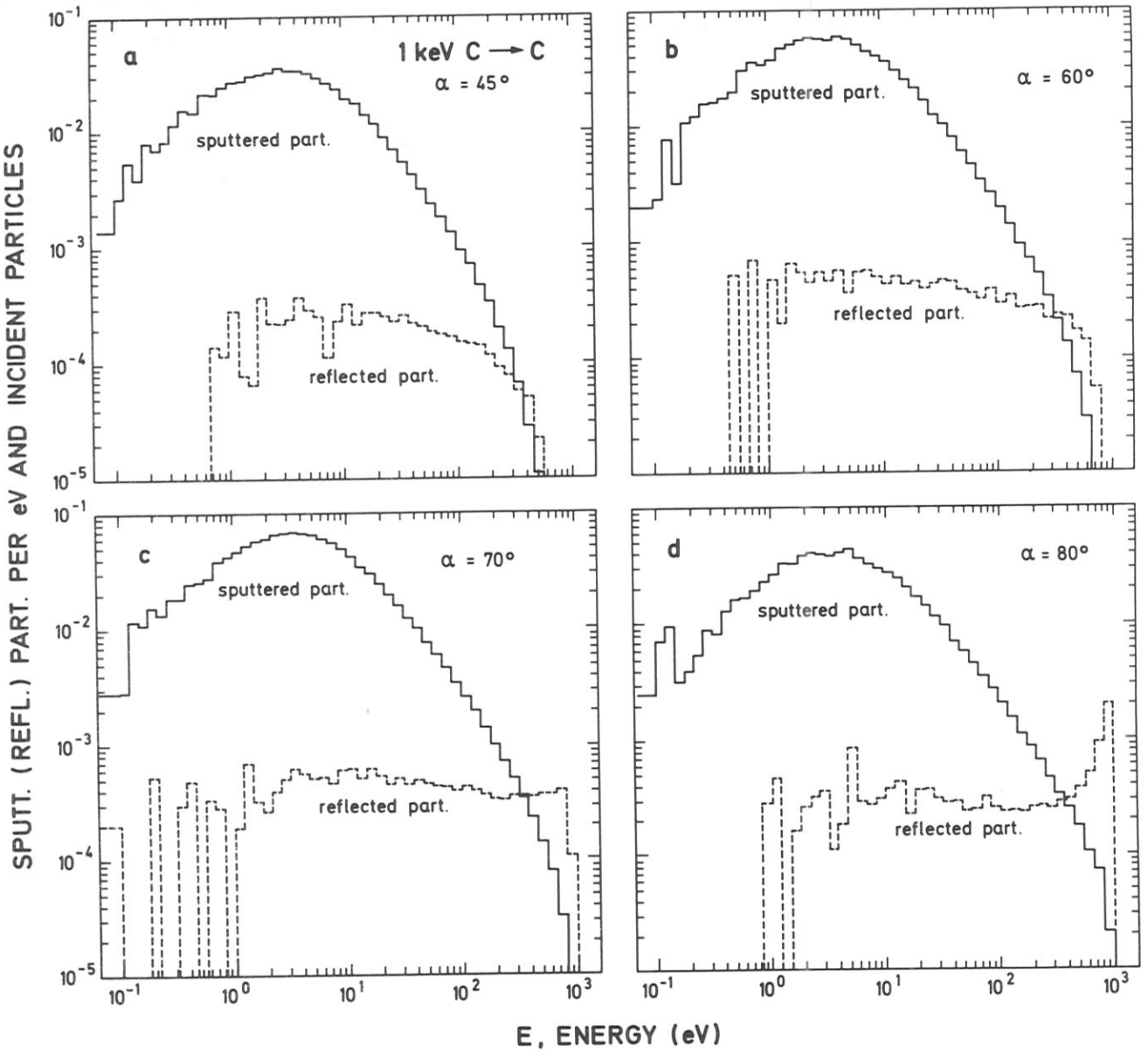
a
1 keV C → C
α = 45°
sputtered part.
reflected part.
b
α = 60°
sputtered part.
reflected part.
c
α = 70°
sputtered part.
reflected part.
d
α = 80°
sputtered part.
reflected part.
SPUTT. (REFL.) PART. PER eV AND INCIDENT PARTICLES
E, ENERGY (eV)

Fig. 14